Various pulsed laser deposition methods for preparation of silver-sensitised glass and paper substrates for surface-enhanced Raman spectroscopy

T. M. Khan[1] · J. G. Lunney[1] · D. O'Rourke[1] · M.-C. Meyer[2] · J. R. Creel[1] · K. E. Siewierska[1]

Abstract

Silver nanoparticle films on glass and paper were prepared using vacuum pulsed laser deposition, and various methods of atmospheric pulsed laser deposition, where ablated material forms a nanoparticle aerosol near the target and is delivered in a gas flow to the substrate. The performance of the films for surface-enhanced Raman spectroscopy (SERS) was investigated using a 10^{-4} M aqueous solution of rhodamine 6G organic dye. The SERS sensitivity was quantified in terms of the apparent enhancement factor and the signal-to-noise ratio. For the films made by supersonic atmospheric pulsed laser deposition, the apparent enhancement factor was found to be 15,000, which is 150 times higher than the value for a commercial silver nanoparticle paper-based substrate. This study demonstrates the utility of atmospheric pulsed laser deposition for the fabrication of noble metal nanoparticle films, and offers new approaches to tailoring the particle morphology for high SERS performance.

1 Introduction

Raman spectroscopy is a useful tool in characterising vibrational and rotational modes of molecules, thus serving as a structural and chemical fingerprint. Intrinsic low sensitivity is a significant limitation of the Raman technique. In the 1970s, surface-enhanced Raman spectroscopy (SERS) was discovered, offering signal enhancements of 10^5–10^6 [1–3]. Since then, intensive research in SERS has led to the development of ultra-high sensitivity, even to the level of single molecule detection [4–6].

The two mechanisms at play in SERS are localised electromagnetic field enhancement and chemical enhancement. The first mechanism is due to the excitation of a surface plasmon resonance (SPR) at the interface between air and a nanotextured metallic surface. The noble metals, such as silver (Ag) and gold (Au) are most commonly used [7, 8]. The nanotexture is often obtained by depositing nanoparticles (NPs) with diameters of 1–100 nm on a dielectric substrate. Relatively, close packing of the NPs leads to regions of high localised electric field enhancement between NPs known as 'hotspots'. While the plasmonic field enhancement is often the dominant contribution to SERS, there is also a contribution from chemical enhancement. This is related to the transfer or exchange of charges between the NP and the adsorbed dye molecules at local atomic structures known as "active sites". The enhancement is a result of a larger Raman scattering cross-section of the molecule–metal system, as compared to the molecule alone, due to the changes in the charge polarizability of the molecule–metal system [9, 10]. Raman scattering is also enhanced by working in the resonant Raman scattering regime of the molecule. The disadvantage of resonant Raman scattering is that the fluorescence will also be significantly enhanced, especially in fluorescent molecules, which can obscure the Raman peaks. However, if the molecules are in a close proximity to noble metal NPs such as Au or Ag, the fluorescence may be quenched via non-radiative energy transfer. This can be facilitated by tuning the particle size and distribution in the NP film [11].

A wide variety of physical and chemical techniques have been used to prepare SERS active surfaces based on NP metal films. Among the physical techniques, pulsed laser deposition (PLD) is a relatively simple method for deposition of metal NP films, and offers some control over the particle size distribution and spacing [12, 13].

✉ J. G. Lunney
jlunney@tcd.ie

[1] School of Physics, Trinity College Dublin, The University of Dublin, Dublin, Ireland

[2] Department of Mechanical and Manufacturing Engineering, Trinity College Dublin, The University of Dublin, Dublin, Ireland

Compared to chemical synthesis methods, such as pre-paring colloidal NP solutions and depositing them on a substrate, PLD offers some advantages, particularly with regard to surface chemical contamination. Colloids often form large flake-like aggregates leading to regions of high SERS enhancement, but with a reduction of point-to-point reproducibility [14, 15]. PLD yields NP films with good uniformity, and the film morphology can be controlled to promote formation of 'hotspots' of laser electric field and Raman enhancement between the NPs [16].

Pulsed laser deposition is normally carried out in vacuum, or a low-pressure gas (< 10 Pa), such that the gas weakly influences the expansion of the laser ablation plume. There is renewed interest in APLD, where laser ablation takes place in gas at atmospheric pressure, leading to strong collisional coupling of the ablated material with the ambient gas and confinement of the ablation plume to within ∼ 1 mm above the target surface. It is expected that collisional condensation will lead to formation of a NP aerosol [17]. Recently, the APLD method was used to make nanostructured Au films by placing the substrate near the ablation spot [18, 19]. A flowing gas, or flowing atmospheric plasma, was used to carry the NP aerosol to a substrate placed at up to 30 mm from the ablation point, and the Ag NP films produced were SERS active [20, 21]. Thus, it seems that APLD is a promising technique for the fabrication of NP films with different morphologies, and seems suitable for translation to industrial application.

Here, we report on a comparative study of the SERS performance of Ag NP films made by vacuum PLD and a variety of APLD methods. Scanning electron microscopy (SEM) was used to examine the NP size distribution, and the overall morphology of the film. Optical absorbance spectra were recorded to determine the spectral position and shape of the SPR. The SERS performance of the various NP films was measured using the organic fluorescent dye R6G. The excitation wavelength of 532.23 nm was chosen to overlap with the peak of the absorption of R6G to ensure resonant Raman scattering. In this manner, the fabricated Ag NP films were tested for both overall Raman signal enhancement as well as fluorescence quenching. The apparent enhancement factor (AEF) and the signal-to-noise ratio (SNR) were calculated and compared to the values obtained with a commercial paper-based SERS sub-strate supplied by Ocean Optics [22].

2 Methodology

2.1 Fabrication of NP films

Silver NP films were made by several different PLD techniques, as summarised in Table 1. Most of the films were prepared using a high repetition rate (HRR) 20 W, 1060.5 nm, 250 ns fibre laser operating at 33 kHz with a pulse energy of 0.6 mJ. NP films were made on glass for optical absorption and SERS measurements, and on silicon for SEM. Films were also deposited on to VWR 516–0351 filter paper with the following characteristics: 84 g m^{-2} weight, 0.2-mm thickness, and 12–15-μm pore size.

The HRR fibre laser was used for the vacuum PLD NP films, where the ultimate chamber pressure was ∼ 2.4 × 10^{-4} mbar, the peak fluence was ∼ 30 J cm^{-2}, the sub-strate was placed at 7.5 cm from the target, and the deposition time was 600 s. The fibre laser was also used to make films by the atmospheric PLD (APLD) technique [21]. Here, the ablation is done at peak laser fluence of ∼ 20 J cm^{-2} in flowing argon (Ar) at 1 bar. The expansion of the ablation plume is constrained by the gas and a NP aerosol is formed close to the target. This aerosol is entrained in the gas flow and transported to a substrate for deposition. The Ar gas was supplied through a 2.4-mm-diameter tube at a rate of 7 litres per minute (LPM), which produced a flow velocity of ∼ 30 m s^{-1} across the ablation spot, and the substrate was positioned at a distance of 10 mm.

For some depositions, a supersonic gas jet was used to carry the aerosol to the substrate. The supersonic jet was formed in a 2 mm × 2 mm square supersonic nozzle operat-ing at 5 bar pressure of argon, which gave an exit veloc-ity of ∼ 400 m s^{-1}, as compared to the sound velocity of 320 m s^{-1} for Ar at room temperature. The substrate was placed at 10 mm from the ablation spot, and the deposition time was 600 s.

Finally, films were made using plasma-assisted APLD [21]. Here, the ablation was done with a 248 nm, 25 ns excimer laser operating at 10 Hz with a laser fluence of

Table 1 Experimental parameters for various deposition methods

Deposition method	Laser parameters (wavelength, pulse duration, energy, repetition rate, fluence)	Gas	Deposition position and time
HRR vacuum PLD	1060.5 nm, 250 ns, 0.6 mJ, 33 kHz, 30 J cm^{-2}	Vacuum	7.5 cm, 600 s
HRR APLD	1060.5 nm, 250 ns, 0.6 mJ, 33 kHz, 20 J cm^{-2}	Ar, 7 LPM	10 mm, 600 s
HRR supersonic APLD	1060.5 nm, 250 ns, 0.6 mJ, 33 kHz, 20 J cm^{-2}	Ar, 400 m s^{-1}	10 mm, 600 s
Plasma-assisted APLD	248 nm, 20 ns, 60 mJ, 10 Hz, 1.4 J cm^{-2}	Ar DBD plasma, 7 LPM	13 mm, 600 s

1.4 J cm^{-2} on target. The NP aerosol formed near the ablation spot was entrained in the plasma outflow from a home-made atmospheric dielectric barrier discharge (DBD). The DBD was excited by applying 8–10 kV sinusoidal voltage at 20 kHz to electrodes placed on the outside of a 2.4-mm-diameter bore quartz tube. The gas flow was 7 LPM, which corresponds to a flow velocity of ~ 30 m s^{-1} near the tube orifice. As before, the tube orifice was placed near the ablation spot, and the aerosol was carried to the substrate at a distance of 13 mm.

2.2 Film characterisation

A Carl Zeiss Ultra field emission SEM, equipped with an in-lens detector and operated at 10 kV, was used to determine the size and morphology of the NPs deposited on Si and paper. The Feret diameters of NPs were obtained from the analysis of SEM images in ImageJ. The mean particle size was determined by log-normal fitting of the size distribution [20]. The UV/visible optical absorbance spectra of the NP films on glass was measured in the range 300–800 nm with a Cary 50 UV–Vis spectrophotometer, using a bare glass substrate as a reference. These absorbance spectra show the position and strength of the surface plasmon resonance (SPR). These spectra were also used to estimate the mass thickness of the NP films. Paramelle et al. [23] examined the UV/visible absorption properties of Ag NPs of various sizes in liquid suspension. As expected, they observed that SPR wavelength depends on the NP size. However, they also observed that the absorbance at 300 nm is relatively independent of NP size and that the absorbance per mass thickness at 300 nm is 0.015 nm^{-1}. Thus, the measured absorbance in the NP films studied here can be used to estimate the mass thickness, as shown in Table 2.

Table 2 Summary SPR maxima and SERS performance of Ag NP films prepared by various PLD and APLD methods on glass and paper

Deposition method	Substrate	Thickness (nm)	SPR maximum (nm)	AEF	SNR
HRR vacuum PLD	Glass	4.4	500	560	240
HRR APLD	Glass	5.3	420	760	190
HRR supersonic APLD	Glass	7.3	390	15,000	1200
Plasma-assisted APLD	Glass	4.9	430	110	90
HRR vacuum PLD	Paper	–	–	90	70
Ocean Optics	Paper	–	–	100	60

2.3 Raman measurements

The SERS performances of the various NP films deposited on glass and paper substrates were compared by recording Raman spectra of R6G using a Horiba Jobin Yvon LabRAM HR800 spectrometer operating in air at room temperature. To match the absorption band of R6G, the excitation wavelength was chosen to be 532.23 nm, and the laser spot size was ~ 1 μm. The R6G stock solution of 10^{-2} M was prepared by dissolving R6G powder in deionised water. The samples for Raman spectroscopy were prepared by drop-casting 10 μL of 10^{-4} M R6G aqueous solution onto the NP films. The diameter of the droplet formed on the substrates was ~ 6 mm, and the samples were left to dry in a heated enclosure. For evaluation of the apparent enhancement factor (AEF), a reference spectrum was recorded for a 10-μL drop of 10^{-2} M dye solution on a bare glass substrate. The performance of the various PLD fabricated SERS substrates was compared with that of a paper-based commercially available Ag NP SERS substrate from Ocean Optics [22]. All samples were excited with a laser power of ~ 200 μW, except the supersonic APLD sample, which was excited with ~ 15 μW to avoid saturation of the detector. That signal was scaled accordingly to allow for direct comparison with other spectra. Raman emission was collected by a 100× objective lens and dispersed using a 600 lines per mm grating. The Raman shift was calibrated to the 521 cm^{-1} peak of a Si/SiO$_2$ sample. The accumulation time was 10 s, and at each position on the sample, 10 spectra were taken and the averaged spectrum was calculated. In the same manner, spectra were acquired from 10 random locations on each sample, and averaged to account for any variation of dye concentration. The background fluorescence spectrum was fitted with a polynomial of degree 8 and subtracted before analysis of the Raman spectra.

3 Results and discussion

Electron microscopy images of Ag NP films made on Si using HRR vacuum PLD, HRR APLD, HRR supersonic APLD, and plasma-assisted APLD are shown in Fig. 1a–d, respectively. All four techniques led to the formation of NP films, though with quite different morphological characteristics. The film thicknesses were controlled by duration of the deposition time and verified by the absorbance spectra, as shown in Fig. 2. All the films show the SPR absorbance feature, though the wavelength of peak absorbance varies according to the deposition technique used. As discussed above, the optical absorbance at 300 nm was used to estimate the mass thickness of the different films, and the values obtained are shown in Table 2. In the SEM image of a HRR vacuum PLD film (Fig. 1a), a substantial fraction of
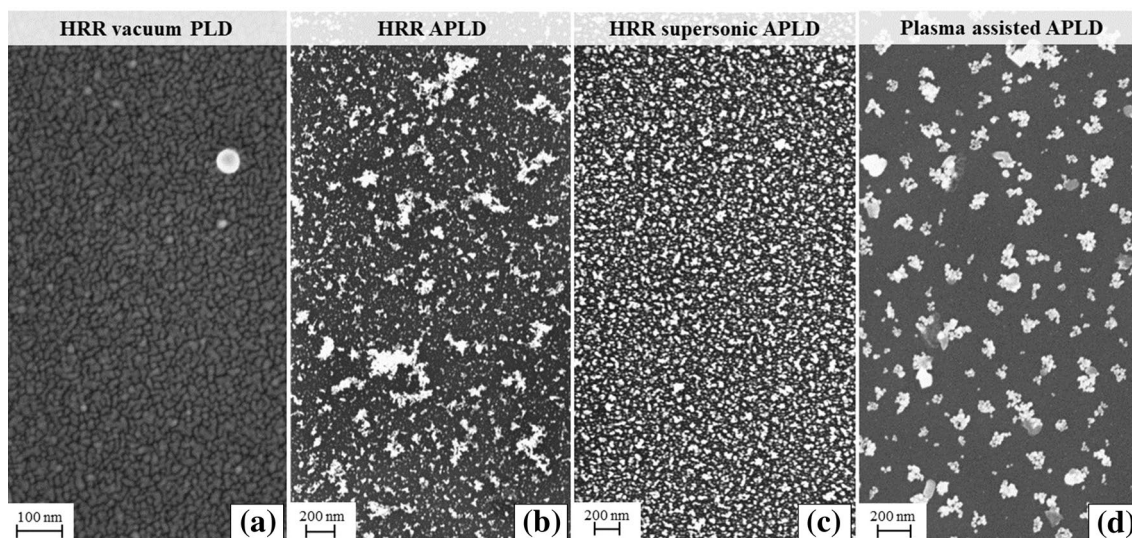
Fig. 1 SEM images of Ag NP films made on Si using: **a** HRR vacuum PLD, **b** HRR APLD, **c** HRR supersonic APLD, and **d** plasma-assisted APLD
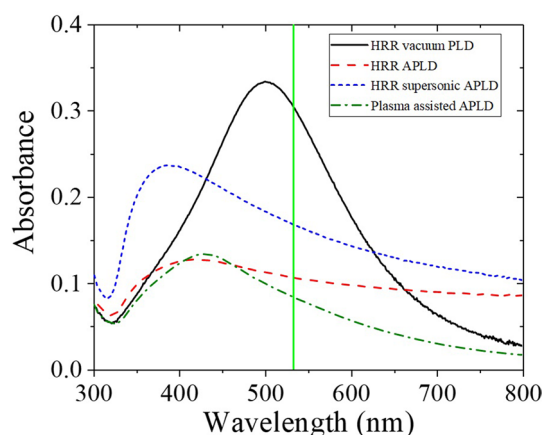

Fig. 2 Optical absorbance spectra of Ag NP films prepared on glass slides by: HRR vacuum PLD, HRR APLD, HRR supersonic APLD, and plasma-assisted APLD. The wavelength of the Raman excitation laser is indicated at 532 nm

elongated NPs can be seen. This is indicative of NP growth by coalescence, as was previously observed in this mass thickness regime [12]. The SPR absorption peak is quite broad with a maximum at 500 nm and FWHM of 220 nm. The HRR APLD film (Fig. 1b) shows a mixed particulate structure; the smaller irregularly shaped NPs have a mean size of 48 (45) nm, where the number in brackets denotes the standard deviation of the distribution. The larger particles seem to be aggregates of the smaller particles, and have dimensions ranging up to 400 nm. The SPR extends across the visible region, perhaps arising from a wide distribution of NP sizes and separations. These films are quite similar to films made using APLD with a 248-nm

excimer laser [20]. The films made by HRR supersonic APLD (Fig. 1c) are more densely packed than for APLD with low flow velocity, and can be described with a single size distribution with a mean size of 45 (38) nm. The SPR has a maximum at 390 nm, but extends again across the visible region. Finally, Fig. 1d shows that the films made by plasma-assisted ns APLD films are comprised of well-separated aggregates of NPs, and relatively few isolated NPs [21]. Here, the SPR is peaked at 430 nm, and is narrower than in the other cases.

The SERS performance was quantified by calculating the apparent enhancement factor (AEF) and signal-to-noise ratio (SNR) values from the measured Raman spectra. The AEF is defined as:

$$AEF = \frac{I_{SERS}}{I_{Ref}} \frac{C_{Ref}}{C_{SERS}},$$

where I_{SERS} is the intensity of the Raman peak at ~1365 cm^{-1}, I_{Ref} is the intensity of the same peak from a substrate without a NP film, C_{SERS} and C_{Ref} are dye concentrations in the samples on NP and bare substrates [9]. The SNR is given by

$$SNR = \frac{S - N}{\sqrt{N}},$$

where S is the intensity of the Raman band at ~1365 cm^{-1} and N is the noise intensity at ~1340 cm^{-1}.

The raw SERS spectra of 10^{-4} M R6G on the various Ag NP films are shown in Fig. 3a, while in Fig. 3b the fluorescent background has been subtracted. For all the
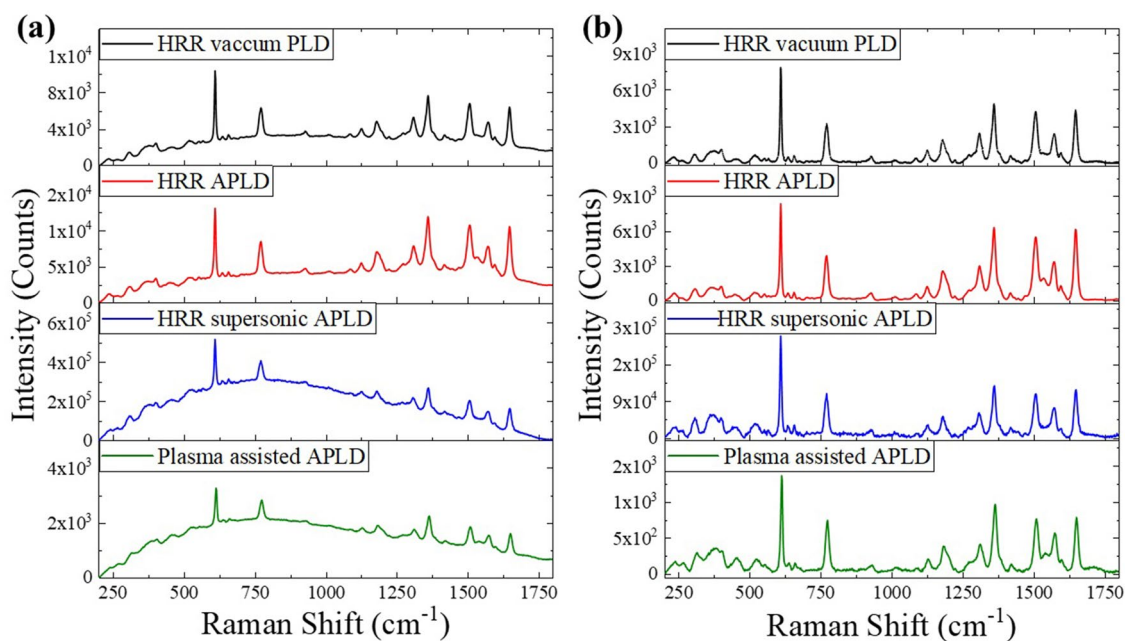
Fig. 3 SERS spectra of 10^{-4} M R6G on Ag NP films on glass slides by: HRR vacuum PLD, HRR APLD, HRR supersonic APLD, and plasma-assisted APLD. **a** Measured spectra before background subtraction, and **b** after subtraction

NP films, well-resolved Raman vibrational modes of R6G are observed within the region of interest from 500 to 1800 cm^{-1}. However, the strength of the Raman signal varies by several orders of magnitude. The AEFs and the SNRs for the various films are tabulated in Table 2 for the Raman line at 1365 cm^{-1} as well as the SPR peak positions from the absorption spectra. Despite having very different morphologies, the AEF values of the HRR vacuum PLD and APLD are quite similar with values of 560 and 760, respectively. The plasma-assisted APLD film showed a lower AEF value of 110, perhaps due to the high degree of NP aggregation caused by the plasma assist. By far, the highest AEF value of 15,000 was recorded for HRR supersonic APLD film. More work would be required to

discern the reasons for this very high value, but it would seem that the lower degree of coagulation, as compared to the HRR APLD film, might be a factor.

As mentioned above, the SERS performance of two paper-based substrates was also investigated and compared with that of the PLD and APLD films. Figure 4a shows an SEM image of the Ocean Optics paper-based SERS substrate made by infusion of Ag NPs. Aggregations of these NPs are clearly seen in the SEM image, together with the paper fibres. Figure 4b shows an SEM image of the substrate made by HRR vacuum PLD on to filter paper. The Ag NPs are visible on the surface of the filter paper. These NPs are about 50 nm in size, with little sign of coagulation.
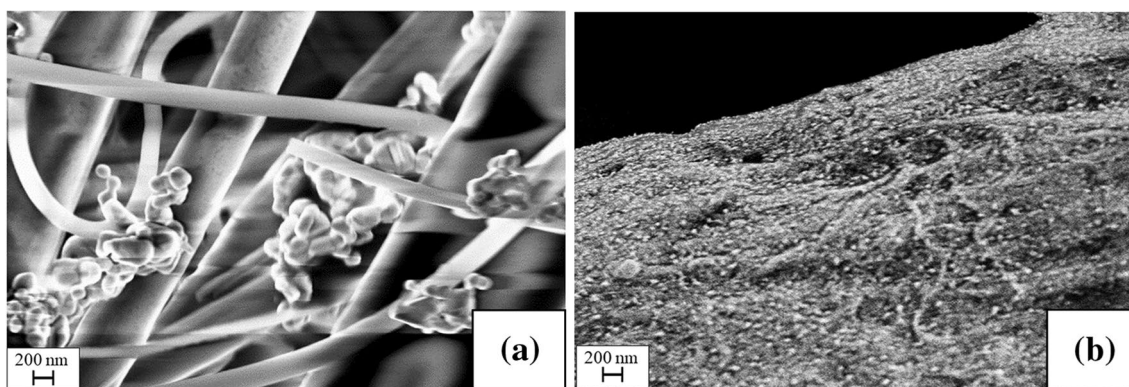

Fig. 4 SEM images of **a** the commercial paper-based Ag SERS substrate, and **b** filter paper coated with Ag using HRR vacuum PLD
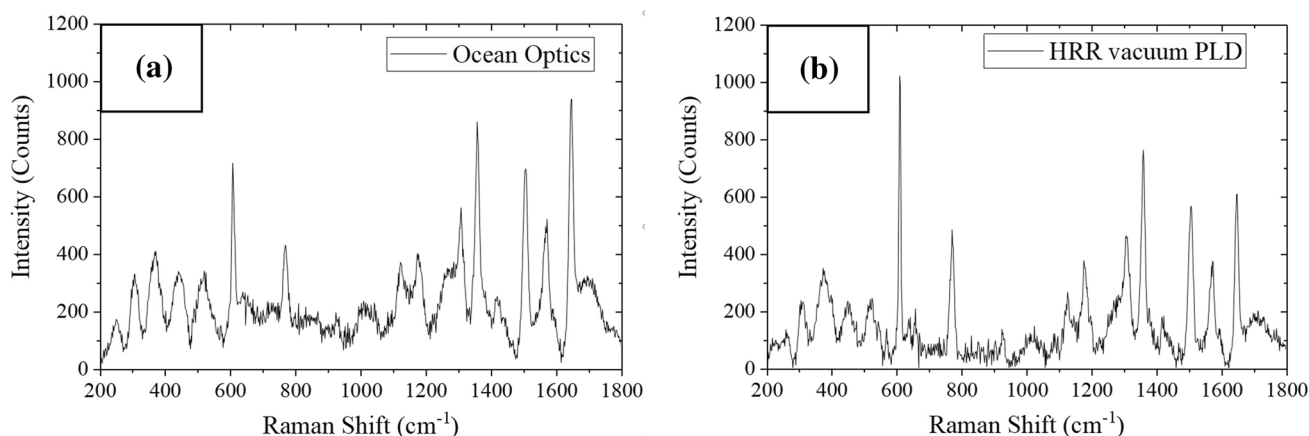
Fig. 5 Raman spectrum of 10^{-4} M aqueous solution R6G measured on **a** Ocean Optics paper substrate infused with Ag NPs, and on **b** a vacuum PLD of Ag on filter paper

Figure 5 shows the Raman spectra (without background subtraction) of a 10-μL drop of 10^{-4} M aqueous solution of R6G on the paper-based substrates; (a) is for the commercial substrate, and (b) is for PLD on filter paper. The expected Raman bands are clearly visible and the calculated AEF and SNR values are summarised in Table 2. Though the NP morphology is quite different in the two substrates, the Raman spectra and SERS performance are remarkably similar.

4 Conclusion

Several different PLD techniques were used to prepare Ag NP films on glass and paper, and their SERS performance was compared. It was found that APLD, where a gas stream is used to carry the ablated material to the substrate, yields highly sensitive substrates. In particular, it was found that NP films made by HRR supersonic APLD are 150× more sensitive than a commercial paper-based Ag substrate. At this stage, many aspects of NP formation and deposition in APLD have neither been investigated in detail, nor is it understood how the relatively high values of SERS sensitivity are related to the nanoscale structure. Nevertheless, it has been clearly demonstrated that APLD offers much scope for the preparation of highly sensitive SERS substrates. It was also demonstrated that vacuum PLD can be used to deposit Ag NPs on to a paper substrate, which has SERS sensitivity similar to a commercial paper SERS substrate.

References

1. M.G. Albrecht, J.A. Creighton, Anomalously intense Raman spectra of pyridine at a silver electrode. J. Am. Chem. Soc. **99**, 5215–5217 (1977)
2. C. D'Andrea, M.J. Lo Faro, G. Bertino, P.M. Ossi, F. Neri, S. Trusso, P. Musumeci, M. Galli, N. Cioffi, A. Irrera, F. Priolo, B. Fazio, Decoration of silicon nanowires with silver nanoparticles for ultrasensitive surface enhanced Raman scattering. Nanotechnology **27**, 375603 (2016)
3. M. Fleischmann, P.J. Hendra, A.J. McQuillan, Raman spectra of pyridine adsorbed at a silver electrode. Chem. Phys. Lett. **26**, 163–166 (1974)
4. B. Sharma, R.R. Frontiera, A.-I. Henry, E. Ringe, R.P. van Duyne, SERS: materials, applications, and the future. Mater. Today **15**, 16–25 (2012)
5. M. Fan, G.F.S. Andrade, A.G. Brolo, A review on the fabrication of substrates for surface enhanced Raman spectroscopy and their applications in analytical chemistry. Anal. Chim. Acta **693**, 7–25 (2011)
6. A. Campion, P. Kambhampati, Surface-enhanced Raman scattering. Chem. Soc. Rev. **27**, 241 (1998)
7. X. Zou, S. Dong, Surface-enhanced Raman scattering studies on aggregated silver nanoplates in aqueous solution. J. Phys. Chem. B **110**, 21545–21550 (2006)
8. S.S.R. Dasary, A.K. Singh, D. Senapati, H. Yu, P.C. Ray, Gold nanoparticle based label-free SERS probe for ultrasensitive and selective detection of trinitrotoluene. J. Am. Chem. Soc. **131**, 13806–13812 (2009)
9. J.J. Gough, K.E. Siewerska, S. Mehigan, D. Hanlon, C. Backes, Z. Gholamvand, B.M. Szydłowska, W.J. Blau, E. McCabe, A.L. Bradley, Influence of graphene oxide/Ag nanoparticle composites on the fluorescence properties of organic dyes. J. Nanosci. Nanotechnol. **17**, 8901–8911 (2017)
10. K. Kneipp, Chemical contribution to SERS enhancement: an experimental study on a series of polymethine dyes on silver nanoaggregates. J. Phys. Chem. C **120**, 21076–21081 (2016)
11. D.L. Dexter, A theory of sensitized luminescence in solids. J. Chem. Phys. **21**, 836–850 (1953)
12. I. Mirza, G. O'Connell, J.J. Wang, J.G. Lunney, Comparison of nanosecond and femtosecond pulsed laser deposition of silver nanoparticle films. Nanotechnology **25**, 265301 (2014)

13. R.W. Eason, D.B. Chrisey (eds.), *Pulsed Laser Deposition of Thin Films: Applications-Led Growth of Functional Materials* (Wiley-Interscience, Hoboken, 2007)
14. R. Tantra, R.J.C. Brown, M.J.T. Milton, Strategy to improve the reproducibility of colloidal SERS. J. Raman Spectrosc. **38**, 1469–1479 (2007)
15. M.A. de Jesús, K.S. Giesfeldt, M.J. Sepaniak, Improving the analytical figures of merit of SERS for the analysis of model environmental pollutants. J. Raman Spectrosc. **35**, 895–904 (2004)
16. C.A. Smyth, I. Mirza, J.G. Lunney, E.M. McCabe, Surface-enhanced Raman spectroscopy (SERS) using Ag nanoparticle films produced by pulsed laser deposition. Appl. Surf. Sci. **264**, 31–35 (2013)
17. T.E. Itina, A. Voloshko, Nanoparticle formation by laser ablation in air and by spark discharges at atmospheric pressure. Appl. Phys. B **113**, 473–478 (2013)
18. N. Nedyalkov, A. Nikolov, P. Atanasov, M. Alexandrov, M. Terakawa, H. Shimizu, Nanostructured Au film produced by pulsed laser deposition in air at atmospheric pressure. Opt. Laser Technol. **64**, 41–45 (2014)
19. R. McCann, C. Hughes, K. Bagga, A. Stalcup, M. Vázquez, D. Brabazon, Pulsed laser deposition of plasmonic nanostructured gold on flexible transparent polymers at atmospheric pressure. J. Phys. D Appl. Phys. **50**, 245303 (2017)
20. T.M. Khan, M.A. Mujawar, K.E. Siewerska, A. Pokle, T. Donnelly, N. McEvoy, G.S. Duesberg, J.G. Lunney, Atmospheric pulsed laser deposition and thermal annealing of plasmonic silver nanoparticle films. Nanotechnology **28**, 445601 (2017)
21. T.M. Khan, A. Pokle, J.G. Lunney, Atmospheric pulsed laser deposition of plasmonic nanoparticle films of silver with flowing gas and flowing atmospheric plasma. Appl. Phys. A **124**, 265301 (2018)
22. Ocean Optics. SERS_Product-Sheet. https://oceanoptics.com/wp-content/uploads/SERS_Product-Sheet.pdf. Accessed 30 July 2018.
23. D. Paramelle, A. Sadovoy, S. Gorelik, P. Free, J. Hobley, D.G. Fernig, A rapid method to estimate the concentration of citrate capped silver nanoparticles from UV–visible light spectra. Analyst **139**, 4855–4861 (2014)